Wood ash-based binders for lightweight building materials: Evaluating the influence of hydraulic lime and cement on the setting and mechanical properties of wood ash pastes

Désiré Ndahirwa, Hafida Zmamou, Hélène Lenormand, Elise Chenot, Sébastien Potel, Nathalie Leblanc

Results in Engineering 24 (2024) 102738

Contents lists available at ScienceDirect

Results in Engineering

journal homepage: www.sciencedirect.com/journal/results-in-engineering

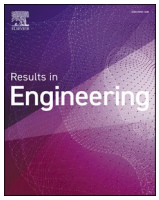

Wood ash-based binders for lightweight building materials: Evaluating the influence of hydraulic lime and cement on the setting and mechanical properties of wood ash pastes

Désiré Ndahirwa [a,*], Hafida Zmamou [a], Hélène Lenormand [a], Elise Chenot [b], Sébastien Potel [b], Nathalie Leblanc [a]

[a] UniLaSalle, Univ. Artois, ULR7519 - Transformations & Agro-ressources, Normandie Université, 3 Rue du Tronquet, 76130 Mont-Saint-Aignan, France
[b] UniLaSalle, B2R (U2R 7511) UPJV-UNIL, 19 Rue Pierre Waguet, 60000 Beauvais, France

ARTICLE INFO

Keywords:
Wood ash
Setting time
Flexural strength
Compressive strength
Wood ash-based pastes

ABSTRACT

The shift from fossil fuels to bioenergy has led to increased wood ash output. Since a large proportion of this waste ends up in landfills, recycling wood ash in construction materials is one of sustainable approaches of managing this by-product. However, the amount of biomass ashes currently recycled in building materials is still limited. This study therefore explored the feasibility of valorising four different types of wood ashes in large quantities in the production of lightweight building materials. Thirty pastes with different levels (80, 90, 95 and 100 wt%) of wood ash and (0, 5, 10 and 20 wt%) of natural hydraulic lime (NHL) or ordinary Portland cement (PC) were developed. Partial replacement of wood ash (WA) by NHL or PC accelerated the setting and improved the mechanical properties of blended pastes. The initial and final setting times decreased with increasing NHL or PC content in the mixes. The strength of the pastes increased with increasing NHL or PC levels and curing time. However, wood bottom ash (WBA) mixes were controversial because their mechanical properties gradually weakened over time. For WA-NHL blends, the 28-day flexural and compressive strength ranged from 0.02 to 1.12 MPa and from 0.05 to 2.59 MPa, respectively. On the other hand, for WA-PC pastes, the flexural and compressive strengths at 28 days varied from 0.07 to 2.72 MPa and from 0.13 to 5.49 MPa, simultaneously. These results prove that wood ash can be used effectively as a main component of binding matrices for lightweight building materials.

1. Introduction

Biomass is the world's largest source of renewable energy, representing 55 % of renewable energy and over 6 % of the global energy supply [1]. In 2018, around 10 million tons of biomass ashes were produced from renewable electricity production alone [2,3]. The annual production of wood ash is estimated at around 18.5 million tons, including 2.42 million tons in Europe [4]. In France, about 92 % of feedstock used for heating is solid biomass which includes wood and its by-products, agricultural and food residues. According to Ref. [5], in France, the gross biomass ash production stood at around 200000 tons in 2015, and was set to surge to 300000 tons by 2020 [5]. Wood ash output has been increasing and this trend is expected to continue due to increasing demand for bioenergy [1,6].

The physicochemical characteristics of biomass ashes vary enormously [7–10]. However, wood ashes typically consist of particles with various sizes and shapes (angular, spherical, irregular). they also contain mineral elements and vital plant nutrients such as calcium, silicon, aluminium, iron, potassium, sodium, magnesium, sulphur, phosphorus, etc., but also large quantities of heavy metals [11–14]. Despite these harmful substances, wood ashes can successfully be recovered in the agriculture, forestry [10] and construction sector [15]. In this last field, an increased interest in wood ash applications in road construction, geopolymers or as an alternative cementitious material to partially replace cement or aggregates in pastes, mortars and concretes has emerged in recent years [11,15–20]. This approach not only reduces the environmental risks associated with wood ash disposal in landfills or random sites, but also contributes to the decarbonization of cement and concrete industry [12]. Despite this, the amount of wood ash used in building materials (i.e.: binders, mortars, concretes) remains limited

* Corresponding author.
E-mail address: desire.ndahirwa@unilasalle.fr (D. Ndahirwa).

https://doi.org/10.1016/j.rineng.2024.102738
Received 18 May 2024; Received in revised form 11 August 2024; Accepted 12 August 2024
Available online 13 August 2024

[15,20–22]. Numerous studies have noted a slight improvement and marginal decrease in the strength of cement-based materials incorporating wood ash (at low levels) and chemical additives (activators, air-entraining agent, water reducing agent, plasticizers, etc.) [23–25]. Omran et al. [26] studied the behaviour of biomass fly ash (BFA) concretes made by replacing 15–25 % of cement with BFA. In addition to BFA, some concretes contained also a polycarboxylate (PCE)-based high-performance water-reducing admixture (HPWRA). The study revealed that concrete containing 25 % BFA and a higher dosage of PCE-based HPWRA had greater compressive strength, splitting tensile strength and modulus of elasticity than the reference concrete made with 100 % Portland cement, particularly at 91 days and beyond. This was ascribed to densification of the BFA concrete microstructure, reduction of pores in the system and pozzolanic reactivity of BFA as the curing age increased. However, at 91 days, the flexural strength of both concretes was similar. In addition, wood ash has also been reported to improve most of the durability parameters of cementitious materials [25–30].

On the other hand, wood ash reportedly has an adverse impact on the water requirement, workability, consistency, setting and strength development of the cement-based materials. Carević et al. [31] observed an increase in water requirement as the wood biomass ash (WBA) content increased in cementitious composites. The study also demonstrated that replacing cement with 5, 10 and 20 % WBA levels lead to a decrease in consistency and workability of mortars due to the morphology of WBA particles and the high alkali content, loss on ignition (LOI) and content of heavy metals. Elinwa and Mahmood [32] investigated the rheological and mechanical properties of concrete mixes made by replacing cement with sawdust ash at different fractions ranging from 0 to 30 %. The study revealed an increase in the water required to achieve the desired consistency, an extension of setting time and a decrease in workability and slump as the percentage of sawdust ash in the mix increased. The compressive strength at 28 days decreased from 23.12 MPa for the control mix (without sawdust ash) to 8.76 MPa for the mix containing 30 % sawdust ash.

Abdullahi [17] studied the behaviour of wood ash/PC concretes, produced by substituting cement with 0, 10, 20, 40 wt% wood ash. The author found that wood ash is slightly pozzolanic, and that water demand and setting time increase with increasing ash content. The initial and final setting times increased from 100 min to 160 min respectively for the control paste to 436 min and 789 min simultaneously for the paste with 40 % wood ash. The study also revealed that compressive strength decreased with increasing ash content but increased over time. Similarly, Ban and Ramli [29] observed a minor increase in water demand to achieve standard consistency and delayed setting of cement pastes following partial replacement of cement with 16 % high-calcium wood ash.

Kula et al. [33] and Wang et al. [34] ascribed the slow setting of cement mixtures blended with wood fly ash, coal fly ash and bottom ash to the higher ratio of ash replacing cement, the chemical and physical characteristics, especially the ash fineness and free lime (CaO) content in the mixtures. Berra et al. [11] attributed prolonged setting time of pastes with 15–30 wt% wood fly ash as a cement replacement to high levels of sulphate and heavy metals in wood fly ash. Furthermore, it has also been reported that a high unburnt content prevents wood ash from solidifying in contact with water [35].

Focusing on mechanical performance, Table 1 presents some previously published data on the flexural and compressive strengths of pastes

Table 1
Reported flexural and compressive strength of the pastes and mortars containing wood ash at 28 days.

WFA (%)	PC (%)	Other SCM (%)	R_f (MPa)	R_c (MPa)	Produced material	Reference
100	0	–	–	≈0.6	Paste	[36]
100	0	–	–	≈0.7		
100	0	–	–	3		
100	0	–	–	6		
0	100	–	9.5 ± 0.6	61.7 ± 2.3	Mortar	[37]
10	90	–	8.8 ± 0.7	58.2 ± 2.4		
20	80	–	8.7 ± 0.8	54.3 ± 3.2		
30	70	–	8.1 ± 0.6	49.1 ± 2.7		
40	60	–	8.1 ± 0.3	42.7 ± 3.4		
50	50	–	6.4 ± 0.5	24.4 ± 1.8		
60	40	–	4.9 ± 0.3	19.4 ± 2.3		
70	30	–	4.2 ± 0.4	13.1 ± 1.3		
20	80	–	3.63–4.16	42.45–46.08	Mortar	[30]
30	70	–	3.57–4.50	32.20–50.19	A Glenium 26 SCC superplasticizer was used	
20	70	MK: 10	6.34–7.28	36.36–41.81		
0	100	–	–	≈46	Mortar	[11]
15	85	–	–	≈39-40		
30	70	–	–	≈38-39		
0	100	–	–	78 ± 4	Mortar cured in water at room temperature	[38]
5	95	–	–	71 ± 5		
10	90	–	–	62 ± 8		
20	80	–	–	49 ± 4		
30	70	–	–	42 ± 4		
WBA (%)						
0	100	–	11.1 ± 1.3	49.5 ± 1.8	Mortar	[24]
5	95	–	10.4 ± 0.4	47.5 ± 1.3		
10	90	–	10.1 ± 1.0	44.3 ± 2.1		
5	95	–	–	82 ± 4	Mortar cured in water at room temperature	[38]
10	90	–	–	74 ± 4		
20	80	–	–	66 ± 4		
30	70	–	–	57 ± 4		
A blend of WFA and WBA (%)						
0	100	–	9.9	61.3	Mortar cured in a highly humid environment for 24h (approx. 98%RH) and in water having a temperature of (23 ± 2)°C for 27 days	[22]
10	90	–	10.3	64.5		
15	85	–	9.8	58.4		
20	80	–	9.4	56.3		

Note: WFA: wood fly ash; WBA: wood bottom ash; PC: ordinary Portland cement; SCM: supplementary cementitious materials; MK: metakaolin.

and mortars incorporated with wood ash (i.e., wood fly ash, wood bottom ash). The wood ash inclusion appears to alter the above strength parameters, as they decrease with increasing levels of ash in the mix.

The reduction in strength of cementitious materials blended with wood ashes is due to multiple factors, including low rate of hydration [39,40], low reactivity of wood ashes, etc. In terms of chemical interactions, wood ash can react either through its hydraulic properties or its pozzolanic properties. However, depending on the oxide components, some ashes may possess both or one of the mentioned properties. Sigvardsen et al. [2] have studied two wood ashes originating from wood chips combustion by grate and circulating fluidised bed combustion, and the authors found that both wood ashes had no pozzolanic properties but did have hydraulic properties.

Ohenoja et al. [36] investigated the reactivity and self-hardening properties of fly ash derived from the combustion of different biomass: paper industry, forest industry residues and various wood wastes. Their study revealed that the compressive strength of fly ash pastes was low in the short term (0.6–6 MPa at 28 days), but due to continuous self-hardening reactions, it gradually increased to between 3 and 11 MPa after 1 year. Zmamou [41] also mixed 90–100 % paper fly ash with 0–10 % PC and found that both pastes containing 90 and 95 % paper fly ash had equal compressive strength (2.6 MPa), while that of control paste (100 % paper fly ash) dropped to 2.1 MPa. To the authors' knowledge, apart from these two studies, no published study has attempted to massively use biomass ash in large quantities into a material. Further data is therefore needed to develop these new materials.

Previous research has focused on adding wood ashes at a limited level (<50 % by weight of cement), mainly to avoid compromising the technical properties of the final materials. Nevertheless, as the demand for bioenergy continues to expand, and thus the production of ash, the construction sector needs to increase the amount of biomass ash it recycles. Biomass ash-based materials could be suitable for applications such as non-load-bearing walls, building insulation, etc. Moreover, scant attention has been paid to the hardening and mechanical properties of materials in which wood ash is dominant and blended with commercial binders, such as natural hydraulic lime (NHL3.5) and ordinary Portland cement (CEM II/B-LL 32.5N), at low levels (less than 20 % by weight of ash).

Therefore, this study investigates the feasibility of utilizing four types of wood ashes as alternative eco-friendly binders for lightweight building materials. Wood ash was the main mix constituent, representing 80 to 100 wt%. While, natural hydraulic lime (NHL) and ordinary Portland cement (PC) were added separately to partially replace the ash at various levels (0, 5, 10, 20 wt%). The hardening and strength development of the wood ash-NHL or wood ash-PC blends were investigated via the Vicat test (on the fresh pastes) and mechanical tests: flexural and compressive strength (on the hardened pastes) at different curing ages (7, 14 and 28 days). Meanwhile, the influence of NHL and PC on the bulk density of the resulting blends was also evaluated.

2. Experimental procedure

2.1. Materials

Four types of wood ashes were used in the preparation of the pastes (see Fig. S1 in supporting information (SI)). The wood fly ash (WFA_3) and wood bottom ash (WBA), originated from combustion of wood pallets, were supplied by Veolia. The other two batches of wood fly ash, named WFA_8 and WFA_9, were provided by a local biomass heating plant known as Coriance (Mont-Saint-Aignan) Energie Verte (MAEV). The latter is equipped with boilers with a power input of 6 and 8 MW. The feedstocks are burnt in the furnace at high temperatures (900–1100 °C). Biomass fuels used include a range of wood chips (forestry wood chips, bocage wood chips, removal from the waste status (SSD) wood chips class A, pallet shavings), wood bark, etc., mainly from the departments of Orne and Calvados, France.

Furthermore, two commercial binders, namely natural hydraulic lime (Saint Jacques PRB hydraulic lime NHL3.5) designated NHL, and ordinary Portland cement (Cement Pro CEM II/B-LL 32.5N) denoted PC, complying respectively to NF EN 459-1 and NF EN 197-1, were introduced to partially replace wood ash.

2.2. Characterization methods

The wood ash samples (WFA_3 and WBA) were received in the form of slurry. Therefore, before being used, they were dried in a ventilated oven at 105 °C for 48h to remove excess moisture and ground with a hammer and passed through a 500 μm aperture sieve to extract large ash particles and carbonaceous matter. On the other hand, WFA_8 and WFA_9 were supplied in a dry state as fine powders and used without any treatment.

The physical properties of wood ashes (WA), NHL and PC, the particle size distribution (PSD) was measured on powder samples soaked in Milli-Q water under agitation, using a Malvern Mastersizer 2000 laser diffractometer equipped with a hydro 2000 MU dispersion unit. Bulk and skeletal densities of all raw materials were measured with a glass cylinder according to Ref. [42] and a pycnometer operating under argon, respectively. Subsequently, their pH was determined by WTW and Mettler Toledo SevenMulti pH-meters according to Refs. [43,44]. For each sample, three measurements were taken to determine the average bulk density and pH. The average skeletal density was obtained from nine replicates.

The chemical composition of WA, NHL and PC was determined by inductively coupled plasma-atomic emission spectroscopy (ICP-AES) and X-ray fluorescence (XRF). XRF was used on selected samples to verify ICP-AES results. The loss on ignition (LOI) of wood ashes, PC and NHL was determined by taking 1g of sample and calcinating it in a muffle furnace (Nabertherm) at 950 °C for 15 min according to Ref. [45]. The pozzolanic activity of WFA_8 was measured by the modified Chapelle test as per NF P18-513 [30,37,46,47]. The experimental protocol is as follows: 1g of WFA_8 was mixed with 2g of calcium oxide (CaO) and 250 mL of distilled water. The solution was then boiled at 90 °C for 16h with continuously stirring (400 rpm) in a glass Erlenmeyer flask connected to a reflux condenser to prevent water loss. After 16h, the Erlenmeyer containing the solution was cooled down at ambient temperature in tap water.

Moreover, a solution of 61.7g of sucrose 0.7 mol/L and 250 mL of distilled water was added to the cooled WFA_8 and CaO solution. The newly formed solution was agitated for 15 min and filtrated with help of a Buchner filter. A filtrate of 200 mL was taken, and each 25 mL of this filtrate was titrated with hydrochloric acid (HCl 0.1(N)) using 2–3 drops of phenolphthalein as an indicator. Ultimately, the amount of fixed calcium hydroxide $Ca(OH)_2$ was calculated based on the volume of HCl solution added, as shown in equation (1).

$$P = 2 \times \frac{V_{1-} V_2}{V_1} \times \frac{74}{56} \times 1000 \quad (1)$$

where P is pozzolanic activity of wood fly ash, expressed in mg $Ca(OH)_2$ fixed by g wood fly ash; V_1 is volume of HCl 0.1N required to titrate 25 mL of the filtrate obtained without wood fly ash (blank test); V_2 is volume of HCl 0.1N required to titrate 25 mL of the filtrate obtained with wood fly ash. It should be noted that the pozzolanic activity reported in this study is an average value obtained from three repetitions.

The morphology of the wood ashes was evaluated with a scanning electron microscopy SEM (JEOL JSM-IT100). Observations were made on a small quantity of the powder sample dispersed on a carbon double-sided sticker covering the sample support. SEM micrographs were obtained in high-vacuum (HV) mode using a secondary electron detector (SED) with an energy of 5 kV and a distance (WD) of 12 mm.

Thermogravimetric analysis TGA (NETZCH-TG 209 F1) was used to study the thermal stability and composition of wood ashes. The tests

were carried out on powder samples with a mass of 20–40 mg, in an argon atmosphere, at a heating rate of 10 °C/min and over a temperature range from 25 to 1000 °C. At least one duplicate was analysed for each sample.

The mineralogical composition, especially the crystalline phases of all raw materials, was assessed using a Bruker D8 Advance X-ray diffractometer. The latter had 2 Theta (θ) configuration, uses a copper anode Ni-filtered Cu Kα radiation generator (λ = 1.540 Å) at 40 kV & 40 mA (primary soller slit of 2.5° and divergence slit of 0.6 mm; secondary soller slit of 2.5°) and was equipped with LynxEye OD detector (slit of 0.1 mm and antiscattering slit of 0.6 mm). The double diffraction angle (2θ) ranged from 3 to 70 with step size of 0.015° and acquisition speed of 0.5 s per step. The diffractograms were treated using DIFFRAC.EVA software.

The setting of wood ash pastes was evaluated in accordance with [48] using a manual Vicat apparatus. Due to the longer setting time of wood ash pastes and time constraints, only WFA_8 was considered for this experiment. The initial setting time was achieved at a needle penetration depth of 35 mm. The final setting time was reached when the needle was unable to penetrate the paste by more than 0.5 mm or when the needle penetrated the paste and made a slight imprint on the surface, whereas the circular attachment has not done so. Nine different fresh pastes were assessed and the measurements were carried out nine times for each paste.

The mechanical properties of the blended pastes were measured with a hydraulic press (Shimadzu, model AGS-X) at a loading rate of 0.5 mm/min. Examples of the samples subjected to the flexural and compressive strength tests are shown in Fig.1 (a, b). The three-point flexural strength (R_f) test was carried out on prism specimens (40 × 40 × 160 mm^3). The fragments from the flexural strength testing were cut into 40 × 40 × 40 mm^3 cubes by a Bosch metal saw. The resulting cubic specimens were then used to determine the compressive strength (R_c). The measurements were taken on 3 replicates for R_f and 3 or 4 replicates for R_c at 7, 14 and 28 days.

2.3. Preparation of the mixtures

Thirty different pastes featuring two binary systems, labelled WA-NHL and WA-PC were developed. According to Table 2 (a, b, c), wood ash (WA) was used as the main ingredient (80–100 wt%), while NHL and PC represented a minor fraction (5–20 wt%) of the mixtures.

The dry raw materials were mixed with tap water using a standard mortar mixer (Controlab) as per [49]. The fresh mixes (WFA_8-NHL and WFA_8-PC) destined for measuring setting time were poured into plastic truncated cone molds (height 40 mm, diameter 60 mm at the top and 70 mm at the bottom) and placed on glass plates. On the other hand, those designed for mechanical tests were casted in steel molds (40 × 40 × 160 mm^3) and compacted using a mini-proctor with a compaction energy of 600 kN m/m^3 [50,51]. The specimens were subsequently removed from the molds after 24h of curing. Then, they were placed in the laboratory and cured at ambient temperature and humidity until the test date.

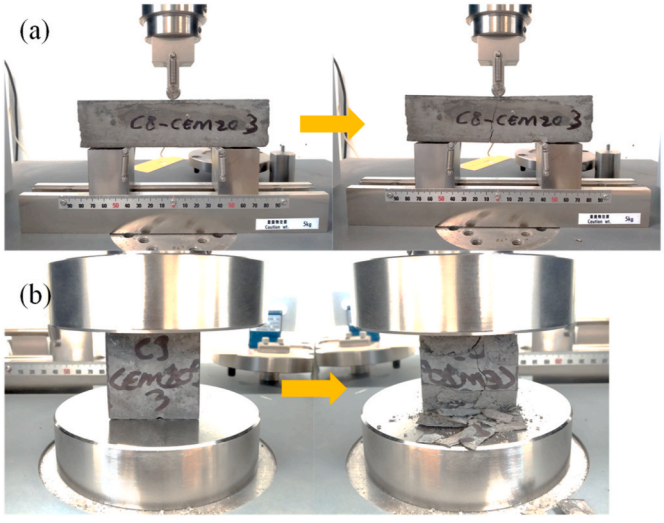

Fig. 1. Examples of samples undergoing flexural (a) and compressive strength (b) tests.

As can be seen in Table 2 (a, b, c), the water/ash ratio (W/A) was 0.5 for pastes containing WFA_8 and WFA_9, while that of pastes made of WFA_3 and WBA was 0.7. These two optimum amounts of mixing water were estimated as follows: numerous wood ash pastes were prepared using different water/ash (W/A) ratios ranging from 0.40 to 0.70. The strength development of the wood ash pastes over time was monitored by measuring the compressive strength at 3, 7, 14 and 28 days. The optimum W/A ratios, shown in Table 2 (a, b, c), were selected based on the 28-day compressive strength and the texture of the fresh pastes. Table S1 (see in SI) summarizes the observations made on the texture of fresh mixes with their respective W/A ratios. For the control mixes comprising 100 wt% NHL and 100 wt% PC, the water/lime and water/cement ratios were 0.5 and 0.35, respectively. Those ratios were selected as they gave pastes with the best texture compared to the other ratios tested.

The water demand varies depending on mix components. The wood ash pastes require more water compared to their cement counterparts. Besides, the WFA_3 and WBA pastes required more mixing water than WFA_8 and WFA_9 mixes. The high water requirement of wood ash pastes can be attributed to high specific surface area, high porosity, irregular particle shape and loss on ignition (LOI) [23,34,36,52].

3. Results and discussion

3.1. Physical and chemical properties of raw materials

3.1.1. Particle size distribution, bulk density and skeletal density

Fig. 2 shows the particle size distribution of raw materials used in this study. Commercial binders (NHL and PC) comprise finer particles compared with wood ashes. The WFA_3 and WBA samples are coarser than WFA_8 and WFA_9. The average particle size (D_{50}) and proportion of ash grains (medium, fine, and very fine) are presented in Table 3. It is worth noting that no coarser particles (diameter >1000 μm) were observed in all wood ashes (WFA_3, WBA, WFA_8, WFA_9).

The bulk and skeletal densities of each raw material were also determined, and the results are given in Table 3. Of all wood ashes, WBA had the highest bulk density. This can be attributed to sand-like structure of the WBA grains, even after manual grinding. The ash samples WFA_3, WFA_8 and WFA_9 exhibited lower bulk densities than NHL and PC. Compared with the literature, the bulk density of wood ashes varies between 490 and 760 kg/m^3 [17,53–55], whilst for NHL, is around 700–846 kg/m^3 [56,57]. For PC, according to the safety data sheet, its bulk density is 900–1500 kg/m^3 [58].

Moreover, the average skeletal density of all raw materials ranged from 2030 ± 7 to 4532 ± 79 kg/m^3, suggesting differences in their porosity. The SEM micrographs of WFA_3, WBA, WFA_8 and WFA_9 are shown in Fig. S2 (see SI). All ash samples show irregular, spherical and fibrous particles of various sizes. Wood bottom ash WBA shows larger coarse particles than other ashes observed. This is consistent with the results previously reported in Fig. 2 and Table 3. Several unburnt wood chips have been also noticed, particularly in wood fly ash samples (WFA_8 and WFA_9).

3.1.2. Chemical composition

The chemical composition of wood ashes, NHL and PC is reported in Table 4. The comparison between ICP-AES and XRF methods revealed remarkable disparities in their results. There are three main raisons for this discrepancy: 1) mineralisation of the sample before ICP-AES

Table 2
Composition of the mixtures.

a. Control pastes.

Mix notation	Substitution (wt.%)	Wood ash (g)	Lime (NHL) (g)	Cement (PC) (g)	W/NHL and W/PC ratios	W/A ratio
100NHL	–	0	1000	0	0.5	–
100PC	–	0	0	1800	0.35	–
100WFA_3	0	1000	0	0	–	0.7
100WBA	0	1000	0	0	–	0.7
100WFA_8	0	1000	0	0	–	0.5
100WFA_9	0	1000	0	0	–	0.5

b. Wood ash pastes incorporated with natural hydraulic lime.

Mix notation	Substitution (wt.%)	Wood ash (g)	Lime (NHL) (g)	W/A ratio
95WFA_3 + 5NHL	5	950	50	0.7
95WBA + 5NHL	5	950	50	0.7
95WFA_8 + 5NHL	5	950	50	0.5
95WFA_9 + 5NHL	5	950	50	0.5
90WFA_3 +10NHL	10	900	100	0.7
90WBA + 10NHL	10	900	100	0.7
90WFA_8 + 10NHL	10	900	100	0.5
90WFA_9 + 10NHL	10	900	100	0.5
80WFA_3 + 20NHL	20	800	200	0.7
80WBA + 20NHL	20	800	200	0.7
80WFA_8 + 20NHL	20	800	200	0.5
80WFA_9 + 20NHL	20	800	200	0.5

c. Wood ash pastes blended with ordinary Portland cement.

Mix notation	Substitution (wt.%)	Wood ash (g)	Cement (PC) (g)	W/A ratio
95WFA_3 + 5PC	5	950	50	0.7
95WBA + 5PC	5	950	50	0.7
95WFA_8 + 5PC	5	950	50	0.5
95WFA_9 + 5PC	5	950	50	0.5
90WFA_3 +10PC	10	900	100	0.7
90WBA + 10PC	10	900	100	0.7
90WFA_8 + 10PC	10	900	100	0.5
90WFA_9 + 10PC	10	900	100	0.5
80WFA_3 + 20PC	20	800	200	0.7
80WBA + 20PC	20	800	200	0.7
80WFA_8 + 20PC	20	800	200	0.5
80WFA_9 + 20PC	20	800	200	0.5

Where A: ash; W: water.

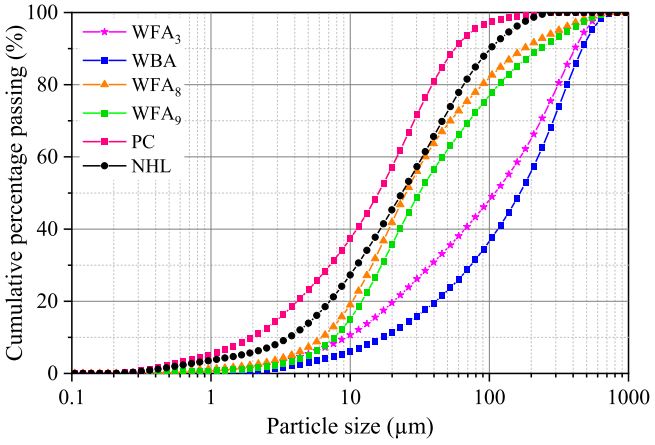

Fig. 2. Particle size distribution of WFA_3, WBA, WFA_8, WFA_9, PC and NHL.

analysis, whereas the XRF was carried out on the sample itself without preparation; 2) the laboratory where ICP-AES was performed provided us with the analysis report covering only the ten oxides listed in the service contract. 3) the calculation uncertainties, as it was assumed that each element was in its oxidised form.

Both methods showed that all samples showed similar oxide components, with levels varying from powder to powder. Regarding ash samples, the major oxide components included CaO, SiO_2, K_2O and SO_3.

Table 3
Physical properties of wood ashes, NHL and PC.

	PC	NHL	WFA_3	WBA	WFA_8	WFA_9
Bulk density (kg/m^3)	1303 ± 12	715 ± 7	631 ± 22	1035 ± 101	374 ± 14	379 ± 14
Skeletal density (kg/m^3)	3078 ± 2	2667 ± 4	2030 ± 7	2318 ± 48	3606 ± 140	4532 ± 79
Average particle size D_{50}	–	–	120.2	181.9	26.3	34.5
Medium particles (80–1000 μm) %	–	–	56.7	68.5	22.1	27.8
Fine particles (2–80 μm) %	–	–	41.9	30.6	75.3	70.6
Very fine particles (<2 μm) %	–	–	1.4	0.9	2.6	1.6

±: Standard deviation.

According to the ICP-AES, CaO represents (17.70–22.50 %), SiO_2 (3.48–17.30 %), K_2O (4.31–9.26 %) and SO_3 (1.52–15.40 %). The sum of pozzolanic oxides %SiO_2, %Al_2O_3 and %Fe_2O_3 in each ash was below 30 %. The LOI of all analysed powders (PC, NHL and wood ashes) range from 13.44 % to 26.54 %. The least amount of organic matter was found in PC, while the highest amount was recorded in WFA_3. When comparing only the wood ashes (WFA_3, WBA, WFA_8 and WFA_9), it is clear that they contain high levels of organic matter (or unburnt carbon) as their LOI values are between 15.52 % and 26.54 %. These LOI rates fall within the range of 1–36 %, reported by Refs. [2,11,13,15,26].

Table 4
Chemical properties of wood ashes, PC and NHL.

Method of analysis	PC		NHL	WFA_3	WBA	WFA_8		WFA_9	
	ICP-AES	XRF	ICP-AES	ICP-AES	ICP-AES	ICP-AES	XRF	ICP-AES	XRF
Components	Content (%)								
SiO_2	15.90	15.72	15.00	7.48	17.30	4.96	15.54	3.48	14.98
Al_2O_3	3.27	3.91	0.30	1.98	3.77	1.25	2.3	1.14	2.15
Fe_2O_3	3.02	2.85	0.18	1.01	2.30	1.39	7.19	2.28	2.39
CaO	43.30	58.18	44.30	22.50	18.20	17.70	37.24	19.50	40.54
MgO	1.00	1.22	0.50	2.63	2.33	2.68	2.55	2.97	3.02
TiO_2	0.20	0.22	0.02	0.14	0.33	0.12	0.18	0.10	0.18
MnO	0.05	0.06	0.01	0.35	0.38	0.95	0.82	1.59	1.34
P_2O_5	0.23	0.21	0.03	2.28	1.77	2.73	1.95	2.76	2.4
K_2O	0.82	1.1	0.06	5.80	4.31	8.14	12.82	9.26	15.01
SO_3	3.01	2.96	0.66	7.36	1.52	15.40	2.9	14.00	1.38
NaO_2		0.04					0.08		0.09
LOI	15.4 ± 0.2*	13.44	22.7 ± 0.1*	26.5 ± 0.1*	17.6 ± 0.9*	16.3 ± 0.2*	15.69	16.2 ± 0.1*	15.52
$SiO_2 + Al_2O_3 + Fe_2O_3$	22.19	22.48	15.47	10.47	23.37	7.60	25.03	6.90	19.52
pH	12.6 ± 0.1		12.7	12.6 ± 0.2	11.4 ± 0.1	12.8		12.8	

±: Standard deviation; *: Determined at UniLaSalle Rouen.

Moreover, the wood ashes investigated were highly alkaline (pH = 11.4–12.8), falling within the pH range of 9–13.5 reported by Refs. [2,8,31,55,59–61]. The higher pH of ashes analysed can be ascribed to the presence of highly alkaline compounds like potassium hydroxide (KOH) and sodium hydroxide (NaOH) [62]. The Chapelle test revealed a fixation of 352 ± 34 mg $Ca(OH)_2/g$ of WFA_8, which is notably lower compared with 1134 mg $Ca(OH)_2/g$ reported by Ref. [22]. The lower pozzolanic activity of WFA_8 is due to multiple factors including its high unburnt carbon levels (Table 4). Owing to time constraints, the pozzolanic activity of WFA_3, WBA, WFA_9 was not determined.

It is noteworthy that, based on the above findings, the analysed wood ashes do not meet all physical and chemical requirements set out in ASTM C618 [63] for coal fly ash and natural pozzolans. However, this does not prevent them from being considered as alternative supplementary cementitious materials in cement-based materials.

3.1.3. *Microstructure and mineralogical composition of wood ashes*

The TGA and DTG curves of wood ashes (WA) are shown in SI Fig. S3 (a, b). Four main endothermic reactions were identified. The mass loss occurring at 25–200 °C was attributed to evaporation of free water, and decomposition of C–S–H and ettringite [64,65]. This peak was more pronounced in WFA_3 and WBA. The second peak was observed at 350–450 °C on samples WFA_8 and WFA_9, and was assigned to the decomposition of portlandite ($Ca(OH)_2$) [65–67]. The large and deep endotherm at 500–800 °C indicated the decomposition of $CaCO_3$ [65,68]. The latter was identified in all WA but the highest intensities were seen on WFA_3 and WFA_9. Finally, the endotherm between 850 and 1000 °C is probably due to the decomposition of dolomite [69,70].

Table 5 and Fig. S4 (shown in SI) show the mineralogical composition, particularly the crystalline phases detected in wood ashes, NHL and PC. The major crystalline phases of WFA_3 are albite ($Na[AlSi_3O_8]$), arcanite (K_2SO_4) and calcite ($Ca(CO_3)$). WBA contains albite ($Na[AlSi_3O_8]$), orthoclase ($K[AlSi_3O_8]$), alite (Ca_3SiO_5), portlandite ($Ca(OH)_2$), calcite ($Ca(CO_3)$) and quartz (SiO_2). The samples WFA_8 and WFA_9 are predominantly composed of albite ($Na[AlSi_3O_8]$), alite (Ca_3SiO_5), calcite ($Ca(CO_3)$), dolomite ($CaMg(CO_3)_2$), portlandite (Ca

Table 5
Crystalline phases detected in PC, NHL and all wood ashes (WFA_3, WBA, WFA_8 and WFA_9) studied.

Compound	PC	NHL	WFA_3	WBA	WFA_8	WFA_9
Albite Na $[AlSi_3O_8]$			++	++	++	++
Alite Ca_3SiO_5	++	++		++	++	++
Alunite $KAl_3(SO_4)_2(OH)_6$		++				
Anhydrite $CaSO_4$						++
Antigorite-T Mg_3 $[Si_2O_5]OH_4$	++					
Arcanite K_2SO_4			++			
Calcite $CaCO_3$	++	++	++	++	++	++
Diopside MgCa $[Si_2O_6]$					++	
Dolomite $CaMg(CO_3)_2$					++	++
Ettringite $Ca_6Al_2(SO_4)_3(OH)_{12}·26H_2O$					+	
Gehlenite Ca_2Al $[AlSiO_7]$						
Goethite FeO(OH)						+
Gypsum $CaSO_4·H_2O$	++					
Lime CaO		+				
Microcline K $[AlSi_3O_8]$		++				
Orthoclase K $[AlSi_3O_8]$				++	++	
Periclase MgO					+	++
Portlandite $Ca(OH)_2$	+	++	+	++	++	++
Quartz SiO_2	Trace	++	+	++	+	++
Sylvite KCl			+		++	++
Syngenite $K_2Ca(SO_4)_2·H_2O$					++	
Variscite $AlPO_4·2H_2O$			++			

Note: ++: major compounds and +: minor compounds.

$(OH)_2$) and sylvite (KCl). WFA_8 also shows important levels of diopside ($MgCa[Si_2O_6]$), orthoclase ($K[AlSi_3O_8]$) and syngenite ($K_2Ca(SO_4)_2{\cdot}H_2O$), whilst WFA_9 exhibits anhydrite ($CaSO_4$), periclase (MgO) and quartz (SiO_2). In addition, the dominant crystalline phases in PC are alite (Ca_3SiO_5), calcite ($CaCO_3$), gypsum ($CaSO_4{\cdot}H_2O$) and antigorite-T ($Mg_3[Si_2O_5]OH_4$) while in NHL the most prevalent phases include alite (Ca_3SiO_5), portlandite ($Ca(OH)_2$), calcite ($CaCO_3$) and microcline ($K[AlSi_3O_8]$).

As shown in Table 5 and Fig. S4 (see in SI), the mineralogical compositions of hydraulic binders, such as PC and NHL, differ from those of the four distinct types of wood ashes evaluated in this study. However, the common mineralogical characteristic of these materials is the presence of calcite, portlandite and quartz, but in varying proportions. The mineralogical compositions of WFA_8 and WFA_9 are comparable. In addition, both ashes had more crystalline phases than WFA_3, WBA, NHL and PC. It is worth mentioning that there was a large variability in the XRD results of the samples, which is related to the chemical composition (Table 4) and thermogravimetric analysis (Fig. S3 given in SI) data.

3.2. Setting time of wood ash pastes

To assess the effect of natural hydraulic lime (NHL) and ordinary Portland cement (PC) on the hardening of wood ash pastes, initial and final setting times were determined. As shown in Fig.3 (a, b), the setting time typically shortens with increasing NHL and PC contents in the mixes.

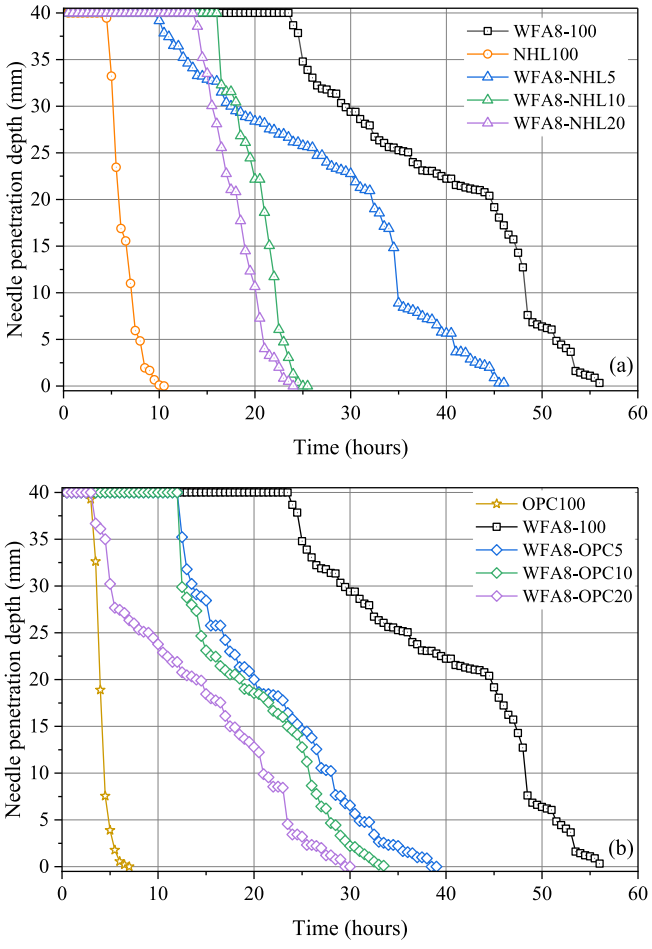

Fig. 3. Initial and final setting times of: (a) WFA_8 pastes blended with NHL and (b) WFA_8 pastes incorporating PC.

For WFA_8-NHL pastes (Fig. 3 (a)), the initial setting time dropped from 25h for the control paste ($100WFA_8$) to 12.5, 16.5 and 14.5h for the WFA_8 pastes containing 5, 10 and 20 % NHL, simultaneously. The final setting time decreased from 56h for $100WFA_8$ to 46, 25 and 24h for the WFA_8 pastes incorporating 5, 10 and 20 % NHL, respectively. WFA_8-NHL blends show faster setting times compared to the paste made entirely from WFA_8 ($100WFA_8$), due to not only the greater reactivity of NHL, but also the presence of alunite ($KAl_3(SO_4)_2(OH)_6$]. In fact, aluminium-containing mineral reacts with Ca^{2+} and SO_4^{2-} to form ettringite. Thus, the rapid generation of ettringite thanks to gypsum and aluminium-containing minerals, improves the setting speed of cementitious materials [71,72].

Regarding WFA_8-PC blends (Fig. 3 (b)), the initial setting time of the control paste ($100WFA_8$) was twice that of pastes incorporating 5 and 10 wt% PC. In addition, the $80WFA_8$-20PC paste achieved an initial setting time of 4.5h, which was closer to the 3.5h recorded for the control paste (100PC). Furthermore, the final setting time decreased from 56h for the control paste ($100WFA_8$) to 38.5, 33.5 and 30h for WFA_8 pastes with 5, 10 and 20 wt% PC respectively. These values are notably greater than for 100PC, which had a final setting time of 7h.

The delayed setting time of WFA_8 pastes was attributed to the physicochemical properties (low reactivity, high lime (CaO) content, high loss on ignition, high levels of sulphate, etc.) of WFA_8, which is in line with the previous studies [11,33–35,73]. In contrast, the accelerated setting, or drastic reduction in setting times, achieved by WFA_8-PC pastes (Fig. 3 (b)) is mainly due to the high reactivity of cement (PC) and its hydration products (i.e., portlandite, ettringite and C–S–H phase). The presence of gypsum in PC (Table 5) also favoured stiffening. In addition, the inclusion of cement in the mixes appeared to reduce the retarding effect of sulphates and organic matter (expressed as LOI) of WFA_8 (Table 4) on setting [11,35]. Furthermore, although the heavy metals concentrations for WFA_8 have not been quantified, previous studies have shown that wood ash generally contains heavy metals and that zinc (Zn), lead (Pb) and copper (Cu) are setting retarders [11,74,75]. It should also be noted that the physicochemical properties (i.e., fineness, bulk density, amounts of SiO_2, Al_2O_3, Fe_2O_3 and CaO) of cement, which differ from those of WFA_8 (Tables 3 and 4), were crucial for setting.

3.3. Mechanical properties of wood ash pastes

3.3.1. Wood ash pastes comprising 0, 5, 10 and 20 wt% natural hydraulic lime

3.3.1.1. Flexural strength. Flexural strengths (R_f) of binary systems made of wood ashes (WA) and natural hydraulic lime (NHL) are shown in Fig. 4. As can be seen, the flexural strength of WFA_3-NHL, WFA_8-NHL and WFA_9-NHL pastes increases with increasing NHL levels and curing time. In contrast, WBA-NHL pastes with 10 and 20 wt% NHL showed higher R_f values at 7 days, but then fell significantly at 14 days and remained more or less stable until 28 days. The mixes with 20 wt% NHL exhibited the highest flexural strengths. However, no significant improvement was observed among WA pastes containing 5 and 10 wt% NHL. The average flexural strengths of pastes at 28 days varied between:

- 0.38 MPa ($100WFA_3$) and 0.44 MPa ($80WFA_3$-20NHL) for WFA_3-NHL pastes;
- 0.02 MPa (95WBA-5NHL) and 0.15 MPa (100WBA) for WBA-NHL pastes;
- 0.65 MPa ($100WFA_8$) and 1.12 MPa ($80WFA_8$-20NHL) for WFA_8-NHL pastes;
- 0.57 MPa ($90WFA_9$-10NHL) and 0.70 MPa ($80WFA_9$-20NHL) for WFA_9-NHL pastes.

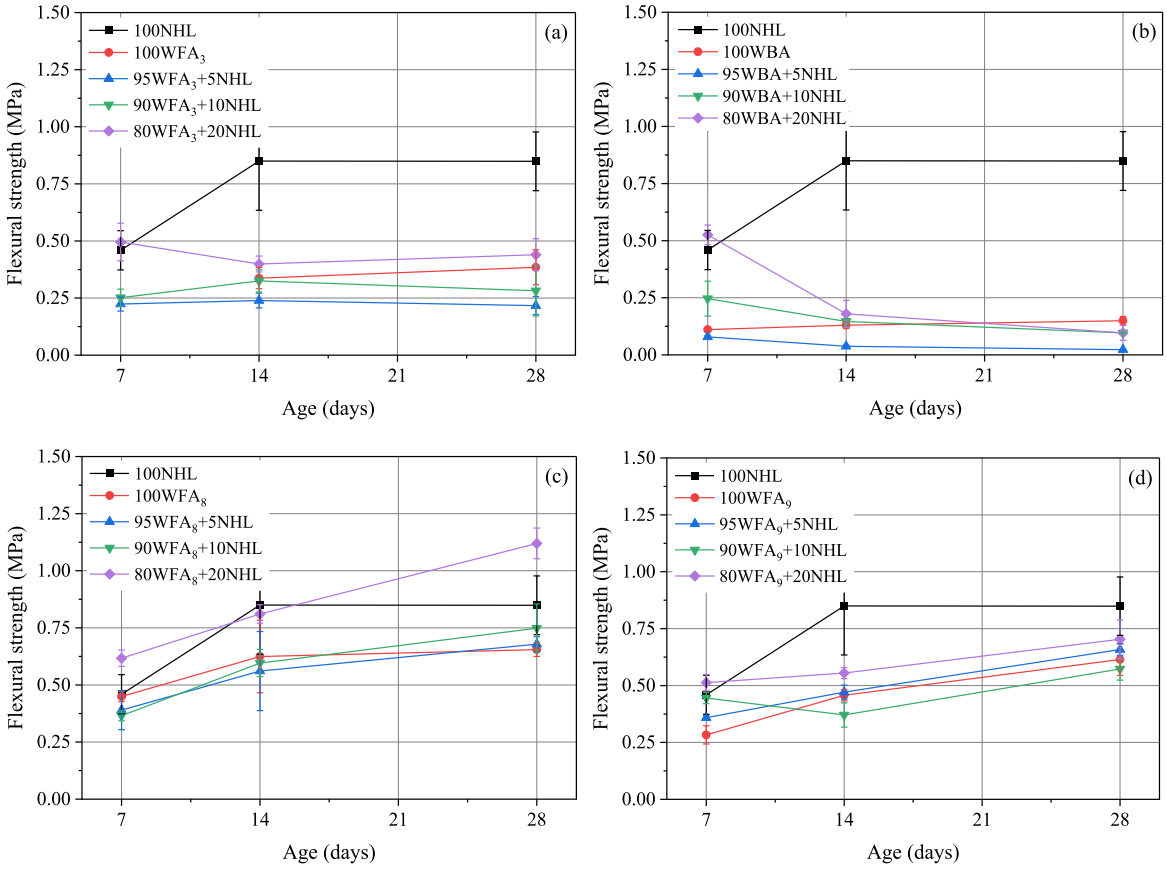

Fig. 4. Flexural strength of wood ash pastes: (a) WFA_3-NHL, (b) WBA-NHL, (c) WFA_8-NHL and (d) WFA_9-NHL.

3.3.1.2. Compressive strength. Fig. 5 reports the compressive strengths of WA-NHL pastes at 7, 14 and 28 days. The results suggest a similar trend to that for flexural strength. Indeed, the compressive strength (R_c) appears to increase with increasing NHL and curing time. In contrast, in case of WBA-NHL pastes, the highest R_c values were reached after only 7 days, but then gradually decreased as the curing time rose. The exact cause of this unusual behaviour could not be determined. However, the low compressive strength of WBA-NHL pastes was ascribed to their unpacked microstructure caused by poor bonding between WBA and NHL due to very low reactivity, high porosity, sandy texture, large grain size and irregular grain shape of WBA. Additionally, it is also speculated that the slow evaporation of water may have increased pores in the paste matrix and thus impaired the mechanical performance of the pastes as the curing time rose.

The average 28-day compressive strength of wood ash pastes ranged between:

- 0.92 MPa ($100WFA_3$) and 2.59 MPa ($80WFA_3$-20NHL) for WFA_3-NHL pastes;
- 0.05 MPa (95WBA-5NHL) and 0.24 MPa (100WBA) for WBA-NHL pastes;
- 0.77 MPa ($100WFA_8$) and 1.82 MPa ($80WFA_8$-20NHL) for WFA_8-NHL pastes;
- 0.72 MPa ($100WFA_9$) and 0.96 MPa ($80WFA_9$-20NHL) for WFA_9-NHL pastes.

Overall, the highest compressive strength (2.59 MPa) at 28 days was obtained from WFA_3-NHL20, suggesting that WFA_3 is more suitable with NHL than other ashes studied.

3.3.1.3. Correlation between compressive strength and bulk density. To further evaluate the mechanical behaviour of WA-NHL pastes, the relationship between their compressive strength (R_c) and bulk density (ρ) at different curing ages (7, 14 and 28 days) was established. As seen in SI Fig. S5, the compressive strength increases with increasing bulk density and curing time. However, it is worth mentioning that bulk density seems to drop slightly with longer curing time. This is typical for all mixes, except WBA pastes, which exhibit the highest R_c and ρ values at 7 days, and the lowest at 28 days.

Overall, the bulk density and compressive strength of the WA-NHL blends were respectively within the range of:

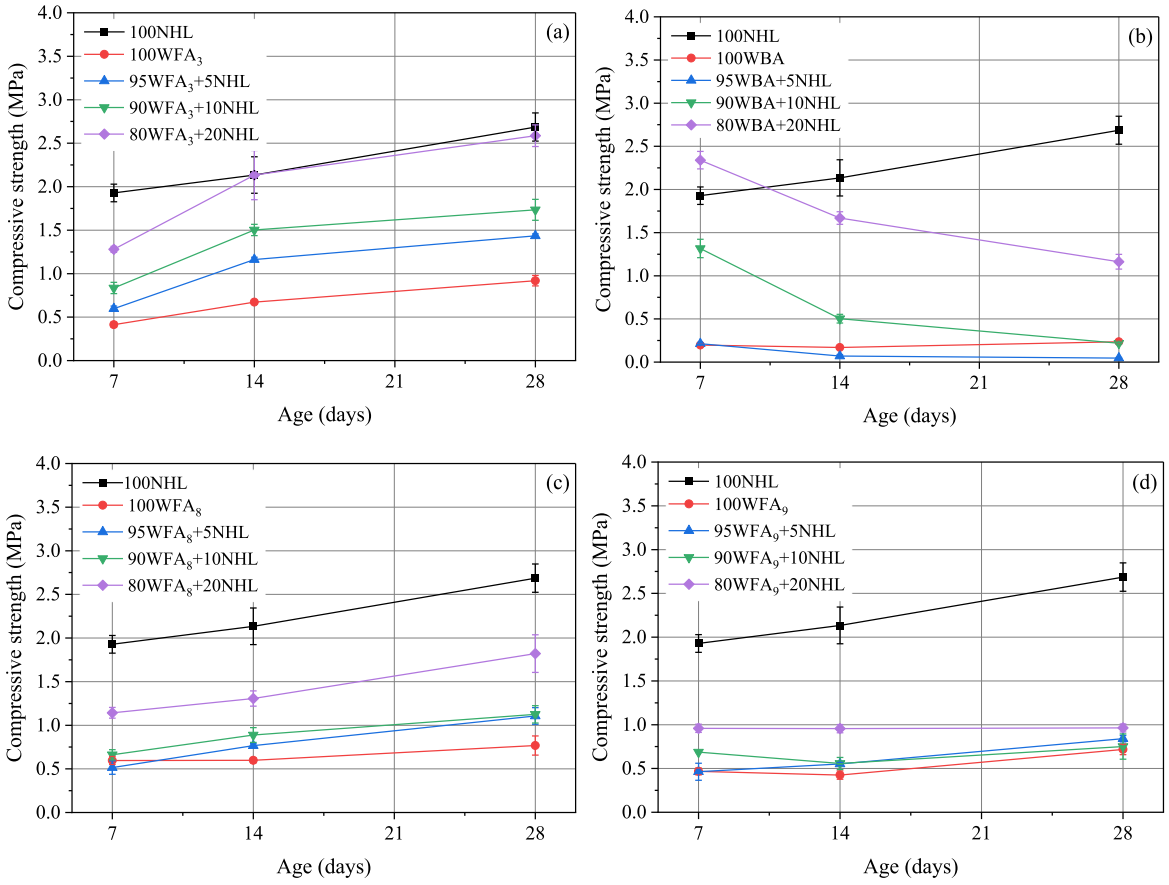

Fig. 5. Compressive strength of wood ash pastes: (a) WFA_3-NHL, (b) WBA-NHL, (c) WFA_8-NHL and (d) WFA_9-NHL.

- 972–1210 kg/m^3 and 0.37–2.77 MPa for WFA_3-NHL pastes;
- 917–1212 kg/m^3 and 0.04–2.46 MPa for WBA-NHL pastes;
- 1218–1407 kg/m^3 and 0.40–2.05 MPa for WFA_8-NHL pastes;
- 1148–1388 kg/m^3 and 0.30–1.03 MPa for WFA_9-NHL pastes.

From this section, it is evident that the addition of NHL significantly improved the strength of WA-NHL blends. This was mainly attributed to the hydration and carbonation of NHL [67]. Also, the increase in strength can be ascribed to the alunite present in NHL that dissolved to release SO_4^{2-} and Al^{3+}, which then reacted with portlandite to form ettringite. In the literature, it has been shown that the higher amount of alunite, the more the amount of ettringite and the greater the strength and expansibility of the pastes [71,76]. Besides, the physical and chemical characteristics of NHL, such as fineness, high bulk density and adequate amounts of SiO_2 and CaO (Fig. 2, Tables 3 and 4) also contributed favourably to the strength of WA-NHL pastes. Finally, the correlation between compressive strengths and bulk densities of wood ash-based hardened pastes indicated a trend consistent with that typically observed for cement-based materials.

3.3.2. Wood ash pastes containing 0, 5, 10 and 20 wt% ordinary Portland cement

3.3.2.1. Flexural strength. The flexural strength (R_f) results of wood ash-PC pastes at 7, 14 and 28 days are given in Fig. 6. Although the overall flexural strength of WA-PC pastes was lower than that of the control paste (made of 100 wt% PC), the addition of PC had a positive impact on the blended pastes. Similar to WA-NHL (stated in paragraph 3.3.1.1), the flexural strength of WA-PC blends was also dependent to the PC levels and curing time. The blends containing WFA_8 and WFA_9 showed better flexural strengths than those of WFA_3 and WBA mixes. At 28 days, the average flexural strength of the wood ash pastes varied between:

- 0.32 MPa (90WFA_3-10PC) and 0.71 MPa (80WFA_3-20PC) for WFA_3-PC pastes;
- 0.07 MPa (95WBA-5PC) and 0.22 MPa (100WBA) for WBA-PC pastes;
- 0.89 MPa (100WFA_8) and 2.72 MPa (80WFA_8-20PC) for WFA_8-PC pastes;
- 0.65 MPa (100WFA_9) and 2.11 MPa (80WFA_9-20PC) for WFA_9-PC pastes.

Compared with the findings reported in paragraph 3.3.1.1, NHL and PC had a negligible influence on the flexural strengths of WFA_3 and WBA pastes. On the contrary, both commercial binders significantly boosted the flexural strengths of WFA_8 and WFA_9 mixes. It should be noted that, overall, PC outperformed NHL.

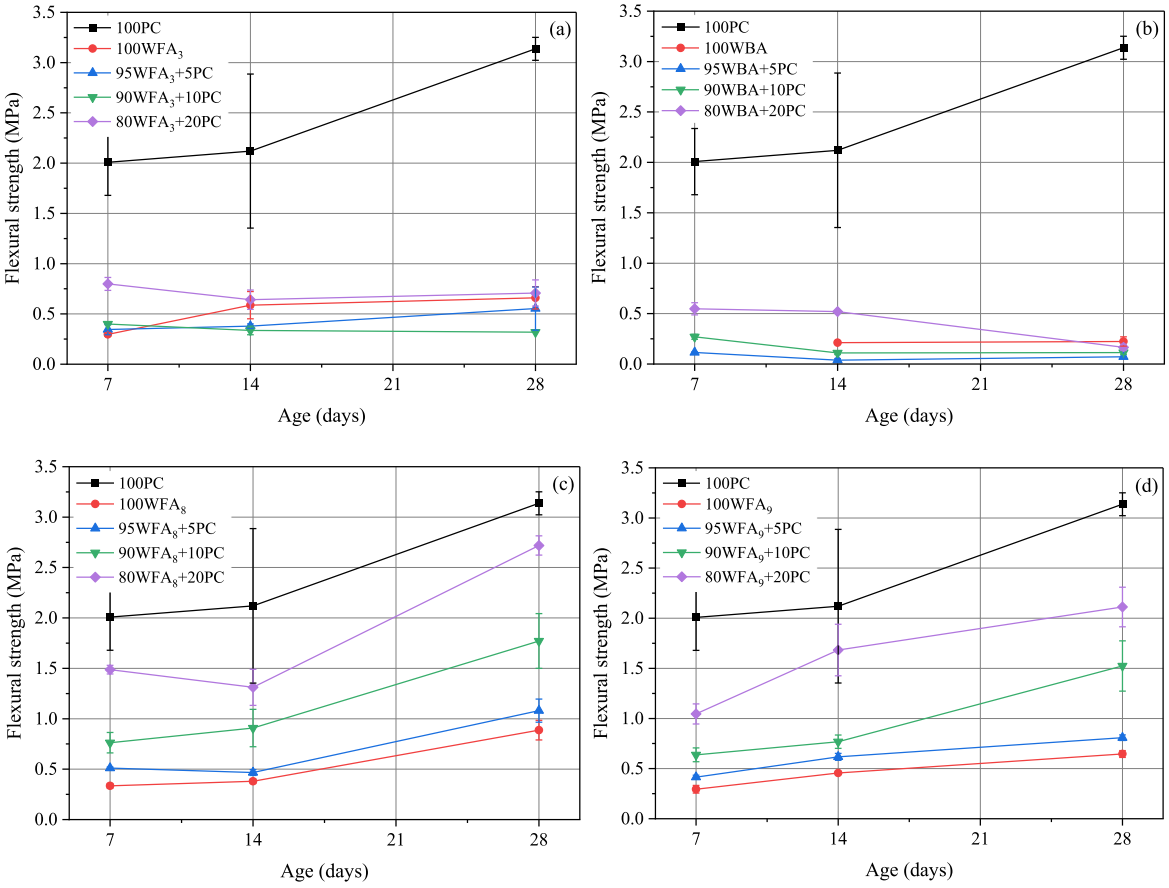

Fig. 6. Flexural strength of wood ash pastes at 7, 14 and 28 days: (a) WFA_3-PC; (b) WBA-PC; (c) WFA_8-PC; (d) WFA_9-PC.

3.3.2.2. Compressive strength. Fig. 7 shows the compressive strength (R_c) of WA-PC binary systems. The 28-day compressive strength of control paste (100PC) was expected to reach 32.5 MPa, but the test was interrupted and stopped at 29 MPa due to the restricted capacity of the hydraulic press load cells. Also, it should be noted that due to a large gap between R_c values of 100PC and wood ash-based pastes, the R_c results of 100PC were excluded from Fig. 7 in order to better represent the compressive strength data of wood ash-containing mixes.

The compressive strengths of WA-PC blends follow a similar trend to that of WA-NHL mixes (mentioned in paragraph 3.3.1.1). It means that the compressive strengths of WA-PC pastes improve as both PC content and curing time increase. However, WBA pastes remain controversial, as their best results in terms of R_c were observed at an early age (7 days), but declined slowly over time. As mentioned earlier in paragraph 3.3.1.2, the underlying cause of the loss of strength is still unknown. Nevertheless, some of the physicochemical features of WBA, namely its sandy texture, large grain size, porosity, lack of compactness, high water demand, poor or even a lack of pozzolanic activity, etc., have been pointed out as major factors contributing to the poor mechanical performance of WBA-based pastes.

On the whole, the average compressive strength of WA-PC pastes at 28 days oscillated between:

- 1.65 MPa (100WFA_3 and 95WFA_3-5 PC) and 3.87 MPa (80WFA_3-20PC) for WFA_3-PC pastes;
- 0.13 MPa (95WBA-5PC) and 2.56 MPa (80WBA-20PC) for WBA-PC pastes;
- 1.40 MPa (100WFA_8) and 5.49 MPa (80WFA_8-20PC) for WFA_8-PC pastes;
- 0.62 MPa (100WFA_9) and 4.01 MPa (80WFA_9-20PC) for WFA_9-PC pastes.

These results are in line with the data previously reported in Refs. [36,41] (0.6–6 MPa). It is also noteworthy that R_c values of WA-PC pastes tend to increase with increasing PC content, and this is coherent with the observations in Refs. [11,37].

3.3.2.3. Relationship between compressive strength and bulk density. Fig. S6 (see SI) plots the compressive strength (R_c) as function of bulk density (ρ) data of WA-PC pastes at 7, 14 and 28 days. WA-PC shows the same trend as previously witnessed for WA-NHL. In fact, the compressive strength WA-PC appears to increase with increasing bulk density and curing time. Also, bulk density slightly drops as curing duration extends.

Ultimately, the bulk density and compressive strength of the WA-PC binary systems respectively fluctuate from:

- 986–1261 kg/m^3 and 0.39–3.99 MPa for WFA_3-PC pastes;
- 895–1272 kg/m^3 and 0.11–4.03 MPa for WBA-PC pastes;
- 1110–1442 kg/m^3 and 0.46–5.75 MPa for WFA_8-PC pastes;

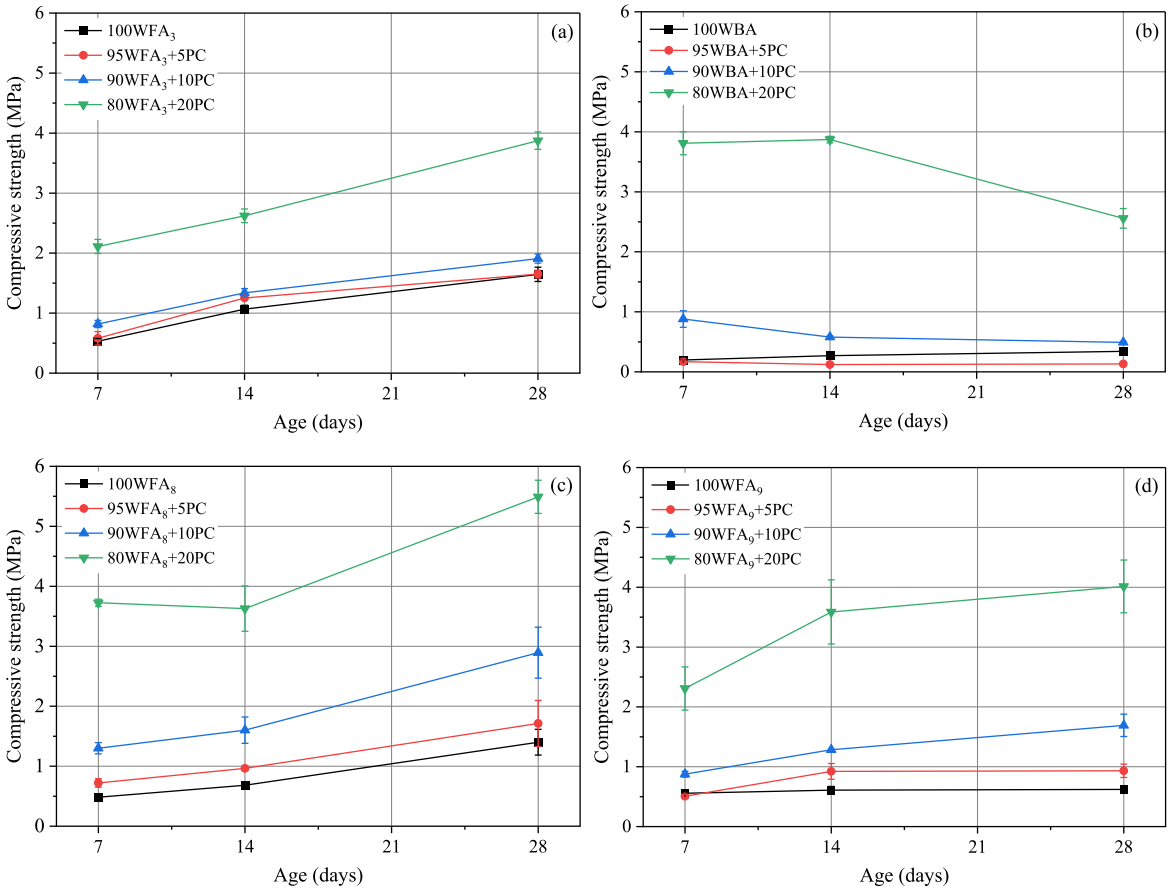

Fig. 7. Compressive strength of wood ash pastes at 7, 14 and 28 days: (a) WFA_3-PC; (b) WBA-PC; (c) WFA_8-PC; (d) WFA_9-PC.

- 1126–1453 kg/m^3 and 0.45–4.35 MPa for WFA_9-PC pastes.

To summarise this section, the improved mechanical performance of WA-PC blends was mainly attributed to the inclusion of cement. Replacing the less reactive wood ashes (WFA_3, WBA, WFA_8 and WFA_9) with a more reactive material, such as cement, played a vital role in the densification and stiffening of the binary systems [73]. Other factors contributing to the strength of WA-PC pastes include (i) the physico-chemical properties (i.e., fineness, high density, high reactivity, etc.): and mineralogical composition (i.e., alite, gypsum, etc.) of cement (ii) cement hydration products (i.e., portlandite, ettringite, C–S–H gel); [77]; (iii) reduction of the adverse effects of setting retarders (i.e., organic matter, sulphates and heavy metals) present in wood ashes after the addition cement. Furthermore, pastes densities have also increased thanks to high bulk density and hydration products of cement. It should be noted that the bulk densities and compressive strengths of WA-PC pastes are dependent on each other.

4. Conclusions

This study investigated the potential for developing alternative binders for lightweight building materials based on wood ashes (WA). Four batches of WA, including three fly ashes (WFA_3, WFA_8 and WFA_9) and one bottom ash (WBA) were evaluated. The physicochemical and mineralogical properties of wood ashes received in dry state (WFA_8 and WFA_9) were different from those of ashes delivered as slurry (WFA_3 and WBA). WFA_8 and WFA_9 were finer and had lower bulk densities, higher skeletal densities and many crystalline minerals than WFA_3 and WBA. No significant differences were noted in the chemical composition of ashes, except a high content of SiO_2 seen in WBA and high alkali levels (i.e., K_2O, SO_3) in WFA_8 and WFA_9. The presence of NHL and PC, which were added as WA partial replacements, offset the negative effects of wood ash constituents and therefore shortened the setting times and significantly improved the mechanical properties of the pastes. For WA-NHL blends, the flexural and compressive strengths vary from 0.02 to 1.12 MPa and 0.05–2.59 MPa, respectively. In the case of WA-PC pastes, the flexural strength ranges from 0.07 to 2.72 MPa, whereas their compressive strength comprises between 0.13 and 5.49 MPa. The optimum mechanical properties were achieved by the wood ash pastes containing 20 wt% PC. Most of the binding matrices developed in this study show sufficient compressive strength to allow the incorporation of plant fibres and particles (hemp, flax, sunflower, etc.). It is therefore feasible to use large quantities of wood ashes in eco-friendly binders for lightweight insulating building materials.

CRediT authorship contribution statement

Désiré Ndahirwa: Writing – review & editing, Writing – original draft, Methodology, Investigation, Conceptualization. **Hafida Zmamou:** Writing – review & editing, Validation, Supervision, Resources, Methodology, Funding acquisition. **Hélène Lenormand:** Writing – review & editing, Validation, Supervision, Resources, Methodology, Funding acquisition. **Elise Chenot:** Writing – review & editing, Validation, Software, Resources. **Sébastien Potel:** Writing – review & editing, Validation, Software, Resources. **Nathalie Leblanc:** Writing – review & editing, Validation, Supervision, Resources, Methodology, Funding acquisition.

Declaration of competing interest

The authors declare that they have no known competing financial interests or personal relationships that could have appeared to influence

the work reported in this paper.

Data availability

Data will be made available on request.

Acknowledgements

This research is part of the first author's PhD thesis, funded by the French environmental and energy management agency (ADEME) through the DIVA project, involving several partners, including PAREXGROUP, UNILASALLE, OVALIE, LA DAUPHINOISE, GDA-LM, ENTPE and FLDI. The authors are grateful to Jean-Baptiste Besnier and Marianne Rosa for their assistance during the laboratory experiments.

Appendix A. Supplementary data

Supplementary data to this article can be found online at https://doi.org/10.1016/j.rineng.2024.102738.

References

[1] IEA Bioenergy, Bioenergy, Energy system overview. More effort needed, IEA, https://www.iea.org/reports/bioenergy, 2022. (Accessed 9 May 2023).
[2] N.M. Sigvardsen, M.R. Geiker, L.M. Ottosen, Reaction mechanisms of wood ash for use as a partial cement replacement, Construct. Build. Mater. 286 (2021) 122889, https://doi.org/10.1016/j.conbuildmat.2021.122889.
[3] IEA Bioenergy, IEA Bioenergy Task 32-Deliverable D7-Options for increased use of ash from biomass combustion and co-firing, IEA. https://www.ieabioenergy.com/wp-content/uploads/2019/02/IEA-Bioenergy-Ash-management-report-revision-5-november.pdf, 2018.
[4] J. Zhai, I.T. Burke, D.I. Stewart, Beneficial management of biomass combustion ashes, Renew. Sustain. Energy Rev. 151 (2021) 111555, https://doi.org/10.1016/j.rser.2021.111555.
[5] D. Boulday, F. Marcovecchio, Valorisation des cendres issues de la combustion de biomasse, Revue des gisements et des procédés associés (No. 14- 0913/1A), CEDEN and LDAR (2016). https://www.record-net.org/storage/etudes/14-0913-1A/rapport/Rapport_record14-0913_1A.pdf.
[6] Ministère de la Transition énergetique, Chiffres clés des énergies renouvelables - Édition 2023. https://www.statistiques.developpement-durable.gouv.fr/edition-numerique/chiffres-cles-energies-renouvelables-2023/, 2023. (Accessed 11 July 2024).
[7] T.A. Abdalla, A.A.E. Hussein, Y.H. Ahmed, O. Semmana, Strength, durability, and microstructure properties of concrete containing bagasse ash – a review of 15 years of perspectives, progress and future insights, Results in Engineering 21 (2024) 101764, https://doi.org/10.1016/j.rineng.2024.101764.
[8] L. Etiégni, A.G. Campbell, Physical and chemical characteristics of wood ash, Bioresour. Technol. 37 (1991) 173–178, https://doi.org/10.1016/0960-8524(91)90207-Z.
[9] A.V. Someshwar, Wood and combination wood-fired boiler ash characterization, J. Environ. Qual. 25 (1996) 962–972, https://doi.org/10.2134/jeq1996.00472425002500050006x.
[10] A. Demeyer, J.C.V. Nkana, M.G. Verloo, Characteristics of wood ash and influence on soil properties and nutrient uptake: an overview, Bioresour. Technol.77 (2001) 287–295.
[11] M. Berra, T. Mangialardi, A.E. Paolini, Reuse of woody biomass fly ash in cement-based materials, Construct. Build. Mater. 76 (2015) 286–296, https://doi.org/10.1016/j.conbuildmat.2014.11.052.
[12] I. Carević, M. Serdar, N. Štirmer, N. Ukrainczyk, Preliminary screening of wood biomass ashes for partial resources replacements in cementitious materials, J. Clean. Prod. 229 (2019) 1045–1064, https://doi.org/10.1016/j.jclepro.2019.04.321.
[13] H.S. Hassan, H.A. Abdel-Gawwad, S.R. Vásquez-García, I. Israde-Alcántara, N. Flores-Ramirez, J.L. Rico, M.S. Mohammed, Cleaner production of one-part white geopolymer cement using pre-treated wood biomass ash and diatomite, J. Clean. Prod. 209 (2019) 1420–1428, https://doi.org/10.1016/j.jclepro.2018.11.137.
[14] I. Obernberger, K. Supancic, Possibilities of ash utilisation from biomass combustion plants, in: Proceedings of the 17th European Biomass Conference & Exhibition, Hamburg, 2009.
[15] K. Tamanna, S.N. Raman, M. Jamil, R. Hamid, Utilization of wood waste ash in construction technology: a review, Construct. Build. Mater. 237 (2020) 117654, https://doi.org/10.1016/j.conbuildmat.2019.117654.
[16] L. Silvestro, T.P. Scolaro, A.S. Ruviaro, G.T.D. Santos Lima, P.J.P. Gleize, F. Pelisser, Use of biomass wood ash to produce sustainable geopolymeric pastes, Construct. Build. Mater. 370 (2023) 130641, https://doi.org/10.1016/j.conbuildmat.2023.130641.
[17] M. Abdullahi, Characteristics of wood ASH/OPC concrete, Leonardo Electron. J. Pract. Technol. (2006) 9–16.
[18] J.-M. Lessard, A. Omran, A. Tagnit-Hamou, R. Gagne, Feasibility of using biomass fly and bottom ashes in dry-cast concrete production, Construct. Build. Mater. 132 (2017) 565–577, https://doi.org/10.1016/j.conbuildmat.2016.12.009.
[19] M. Salvo, S. Rizzo, M. Caldirola, G. Novajra, F. Canonico, M. Bianchi, M. Ferraris, Biomass ash as supplementary cementitious material (SCM), Adv. Appl. Ceram. 114 (2015) S3–S10, https://doi.org/10.1179/1743676115Y.0000000043.
[20] M.N.L. Leroy, K.T.J. Hermann, A.N.E. Rose, N. Joseph, F.M.C. Dupont, N.J.-M. Bienvenu, Density and strength of mortar made with the mixture of wood ash, crushed gneiss and river sand as fine aggregate, MSCE 06 (2018) 109–120, https://doi.org/10.4236/msce.2018.64012.
[21] M. Adamu, A.S. Tifase, O.A.U. Uche, Engineering Properties of Industrial Wood Waste Ash-Concrete, vol. 1 (n.d.).
[22] M. Pavlíková, L. Zemanová, J. Pokorný, M. Záleská, O. Jankovský, M. Lojka, D. Sedmidubský, Z. Pavlík, Valorization of wood chips ash as an eco-friendly mineral admixture in mortar mix design, Waste Manag. 80 (2018) 89–100, https://doi.org/10.1016/j.wasman.2018.09.004.
[23] O.A. Abdulkareem, M. Ramli, J.C. Matthews, Production of geopolymer mortar system containing high calcium biomass wood ash as a partial substitution to fly ash: an early age evaluation, Compos. B Eng. 174 (2019) 106941, https://doi.org/10.1016/j.compositesb.2019.106941.
[24] M. da L. Garcia, J. Sousa-Coutinho, Strength and durability of cement with forest waste bottom ash, Construct. Build. Mater. 41 (2013) 897–910, https://doi.org/10.1016/j.conbuildmat.2012.11.081.
[25] T. Ramos, A.M. Matos, J. Sousa-Coutinho, Mortar with wood waste ash: mechanical strength carbonation resistance and ASR expansion, Construct. Build. Mater. 49 (2013) 343–351, https://doi.org/10.1016/j.conbuildmat.2013.08.026.
[26] A. Omran, N. Soliman, A. Xie, T. Davidenko, A. Tagnit-Hamou, Field trials with concrete incorporating biomass-fly ash, Construct. Build. Mater. 186 (2018) 660–669, https://doi.org/10.1016/j.conbuildmat.2018.07.084.
[27] E.R. Teixeira, A. Camões, F.G. Branco, Valorisation of wood fly ash on concrete, Resour. Conserv. Recycl. 145 (2019) 292–310, https://doi.org/10.1016/j.resconrec.2019.02.028.
[28] C.B. Cheah, M. Ramli, Mechanical strength, durability and drying shrinkage of structural mortar containing HCWA as partial replacement of cement, Construct. Build. Mater. 30 (2012) 320–329, https://doi.org/10.1016/j.conbuildmat.2011.12.009.
[29] C.C. Ban, M. Ramli, Properties of high calcium wood ash and densified silica fume blended cement, Int. J. Phys. Sci. 6 (2011), https://doi.org/10.5897/IJPS11.1485.
[30] T.C. Esteves, R. Rajamma, D. Soares, A.S. Silva, V.M. Ferreira, J.A. Labrincha, Use of biomass fly ash for mitigation of alkali-silica reaction of cement mortars, Construct. Build. Mater. 26 (2012) 687–693, https://doi.org/10.1016/j.conbuildmat.2011.06.075.
[31] I. Carević, A. Baričević, N. Štirmer, J. Šantek Bajto, Correlation between physical and chemical properties of wood biomass ash and cement composites performances, Construct. Build. Mater. 256 (2020) 119450, https://doi.org/10.1016/j.conbuildmat.2020.119450.
[32] A.U. Elinwa, Y.A. Mahmood, Ash from timber waste as cement replacement material, Cement Concr. Compos. 24 (2002) 219–222, https://doi.org/10.1016/S0958-9465(01)00039-7.
[33] I. Kula, A. Olgun, Y. Erdogan, V. Sevinc, Effects of colemanite waste, cool bottom ash, and fly ash on the properties of cement, Cement Concr. Res. (2001) 4.
[34] S. Wang, A. Miller, E. Llamazos, F. Fonseca, L. Baxter, Biomass FLy Ash in Concrete: Mixture Proportioning and Mechanical Properties, 2008, p. 7.
[35] B.-M. Steenari, O. Lindqvist, Stabilisation of biofuel ashes for recycling to forest soil, Biomass Bioenergy 13 (1997) 39–50.
[36] K. Ohenoja, P. Tanskanen, V. Wigren, P. Kinnunen, M. Körkkö, O. Peltosaari, J. Österbacka, M. Illikainen, Self-hardening of fly ashes from a bubbling fluidized bed combustion of peat, forest industry residuals, and wastes, Fuel 165 (2016) 440–446, https://doi.org/10.1016/j.fuel.2015.10.093.
[37] J. Fořt, J. Šál, R. Ševčík, M. Doleželová, M. Keppert, M. Jerman, M. Záleská, V. Stehel, R. Černý, Biomass fly ash as an alternative to coal fly ash in blended cements: functional aspects, Construct. Build. Mater. 11 (2021).
[38] S. Maschio, G. Tonello, L. Piani, E. Furlani, Fly and bottom ashes from biomass combustion as cement replacing components in mortars production: rheological behaviour of the pastes and materials compression strength, Chemosphere 85 (2011) 666–671, https://doi.org/10.1016/j.chemosphere.2011.06.070.
[39] B.D. Ikotun, A.A. Raheem, Characteristics of wood ash cement mortar incorporating green-synthesized nano-TiO2, Int J Concr Struct Mater 15 (2021) 19, https://doi.org/10.1186/s40069-021-00456-x.
[40] A.A. Raheem, B.S. Olasunkanmi, C.S. Folorunso, Saw dust ash as partial replacement for cement in concrete, OTMCJ 4 (2012), https://doi.org/10.5592/otmcj.2012.2.3.
[41] H. Zmamou, Eco-conception de nouveaux agromatériaux à partir de cendre de chaudière biomasse. Relation structures-proprietes, Thèse de doctorat, Université de Rouen, 2015.
[42] S. Amziane, F. Collet (Eds.), Bio-aggregates Based Building Materials: State-Of-The-Art Report of the RILEM Technical Committee 236-BBM, Springer Netherlands, Dordrecht, 2017, https://doi.org/10.1007/978-94-024-1031-0.
[43] A. Behnood, K. Van Tittelboom, N. De Belie, Methods for measuring pH in concrete: a review, Construct. Build. Mater. 105 (2016) 176–188, https://doi.org/10.1016/j.conbuildmat.2015.12.032.
[44] M.N. Haque, O.A. Kayyali, Free and water soluble chloride in concrete, Cement Concr. Res. 25 (1995) 531–542, https://doi.org/10.1016/0008-8846(95)00042-B.
[45] ASTM International C114-04, Standard Test Methods for Chemical Analysis of Hydraulic Cement, 2004.

[46] F. Avet, R. Snellings, A. Alujas Diaz, M. Ben Haha, K. Scrivener, Development of a new rapid, relevant and reliable (R3) test method to evaluate the pozzolanic reactivity of calcined kaolinitic clays, Cement Concr. Res. 85 (2016) 1–11, https://doi.org/10.1016/j.cemconres.2016.02.015.
[47] E. Ferraz, S. Andrejkovičová, W. Hajjaji, A.L. Velosa, A.S. Silva, F. Rocha, Pozzolanic activity of metakaolins by the French standard of the modified Chapelle test: a direct methology, Acta Geodyn. Geomater. (2015) 289–298, https://doi.org/10.13168/AGG.2015.0026.
[48] NF EN 196-3, Methods of testing cement - Part 3 : determination of setting times and soundness, Afnor EDITIONS. https://www.boutique.afnor.org/Store/Preview/DisplayExtract?ProductID=79422&VersionID=14, 2017. (Accessed 10 August 2022).
[49] NF EN 196-1, NF EN 196-1, Méthodes d'essais des ciments - Partie 1 : Détermination des résistances, 2016.
[50] M. Hussain, D. Levacher, N. Leblanc, H. Zmamou, I. Djeran-Maigre, A. Razakamanantsoa, L. Saouti, Reuse of harbour and river dredged sediments in adobe bricks, Cleaner Materials 3 (2022) 100046, https://doi.org/10.1016/j.clema.2022.100046.
[51] S. Seifi, N. Sebaibi, D. Levacher, M. Boutouil, Mechanical performance of a dry mortar without cement, based on paper fly ash and blast furnace slag, J. Build. Eng. 22 (2019) 113–121, https://doi.org/10.1016/j.jobe.2018.11.004.
[52] C.B. Cheah, M.H. Samsudin, M. Ramli, W.K. Part, L.E. Tan, The use of high calcium wood ash in the preparation of Ground Granulated Blast Furnace Slag and Pulverized Fly Ash geopolymers: a complete microstructural and mechanical characterization, J. Clean. Prod. 156 (2017) 114–123, https://doi.org/10.1016/j.jclepro.2017.04.026.
[53] S. Chowdhury, A. Maniar, O.M. Suganya, Strength development in concrete with wood ash blended cement and use of soft computing models to predict strength parameters, J. Adv. Res. 6 (2015) 907–913, https://doi.org/10.1016/j.jare.2014.08.006.
[54] T.R. Naik, Greener concrete using recycled materials, Concr. Int. 24 (2002) 45–49.
[55] R. Siddique, Utilization of wood ash in concrete manufacturing, Resour. Conserv. Recycl. 67 (2012) 27–33, https://doi.org/10.1016/j.resconrec.2012.07.004.
[56] L. Arnaud, E. Gourlay, Experimental study of parameters influencing mechanical properties of hemp concretes, Construct. Build. Mater. 28 (2012) 50–56, https://doi.org/10.1016/j.conbuildmat.2011.07.052.
[57] J. Grilo, P. Faria, R. Veiga, A. Santos Silva, V. Silva, A. Velosa, New natural hydraulic lime mortars – physical and microstructural properties in different curing conditions, Construct. Build. Mater. 54 (2014) 378–384, https://doi.org/10.1016/j.conbuildmat.2013.12.078.
[58] Cimalit Ciment du Littoral, Fiche de données de sécurité, Ciments courants : CEM II 32.5 N. https://media.adeo.com/marketplace/LMFR/80136217/78ad6897-2fb9-436a-bef5-fec824a5c90f.pdf, 2017. (Accessed 15 November 2023).
[59] O. Dahl, H. Nurmesniemi, R. Pöykiö, G. Watkins, Heavy metal concentrations in bottom ash and fly ash fractions from a large-sized (246MW) fluidized bed boiler with respect to their Finnish forest fertilizer limit values, Fuel Process. Technol. 91 (2010) 1634–1639, https://doi.org/10.1016/j.fuproc.2010.06.012.
[60] A.U. Elinwa, S.P. Ejeh, Effects of the incorporation of sawdust waste incineration fly ash in cement pastes and mortars, J. Asian Architect. Build Eng. 3 (2004) 1–7, https://doi.org/10.3130/jaabe.3.1.
[61] J.-M. Mivière, Les Cendres des chaudières automatiques au bois et leurs possibilités de valorisation-Les cahiers du Bois énergie : Fascicule 1. https://www.bois-energie.ofme.org/documents/Environnement/BE66_valorisation_des_cendres.pdf, 2008.
[62] M. Gori, B. Bergfeldt, G. Pfrang-Stotz, J. Reichelt, P. Sirini, Effect of short-term natural weathering on MSWI and wood waste bottom ash leaching behaviour, J. Hazard Mater. 189 (2011) 435–443, https://doi.org/10.1016/j.jhazmat.2011.02.045.
[63] ASTM International C618-03, Standard Specification for Coal Fly Ash and Raw or Calcined Natural Pozzolan for Use in Concrete, 2004.
[64] C.E.M. Gomes, O.P. Ferreira, M.R. Fernandes, Influence of vinyl acetate-versatic vinylester copolymer on the microstructural characteristics of cement pastes, Mater. Res. 8 (2005) 51–56.
[65] K. Ohenoja, J. Rissanen, P. Kinnunen, M. Illikainen, Direct carbonation of peat-wood fly ash for carbon capture and utilization in construction application, J. CO2 Util. 40 (2020) 101203, https://doi.org/10.1016/j.jcou.2020.101203.
[66] G. Puerta-Falla, M. Balonis, G. Le Saout, G. Falzone, C. Zhang, N. Neithalath, G. Sant, Elucidating the role of the aluminous source on limestone reactivity in cementitious materials, J. Am. Ceram. Soc. 98 (2015) 4076–4089, https://doi.org/10.1111/jace.13806.
[67] Ö. Cizer, C. Rodriguez-Navarro, E. Ruiz-Agudo, J. Elsen, D. Van Gemert, K. Van Balen, Phase and morphology evolution of calcium carbonate precipitated by carbonation of hydrated lime, J. Mater. Sci. 47 (2012) 6151–6165, https://doi.org/10.1007/s10853-012-6535-7.
[68] Z. Zhu, H. Chu, M. Guo, M. Shen, L. Jiang, L. Yu, Effect of silica fume and fly ash on the stability of bound chlorides in cement mortar during electrochemical chloride extraction, Construct. Build. Mater. 256 (2020) 119481, https://doi.org/10.1016/j.conbuildmat.2020.119481.
[69] M. Földvári, Handbook of Thermogravimetric System of Minerals and its Use in Geological Practice, Geological Inst. of, Hungary, Budapest, 2011.
[70] M. Samtani, D. Dollimore, K.S. Alexander, Comparison of dolomite decomposition kinetics with related carbonates and the effect of procedural variables on its kinetic parameters, Thermochim. Acta (2002) 11.
[71] M. Katsioti, D. Giannikos, P.E. Tsakiridis, Z. Tsibouki, Properties and hydration of blended cements with mineral alunite, Construct. Build. Mater. 23 (2009) 1011–1021, https://doi.org/10.1016/j.conbuildmat.2008.05.007.
[72] C. Ma, Y. Tan, E. Li, Y. Dai, M. Yang, High-performance grouting mortar based on mineral admixtures, Adv. Mater. Sci. Eng. 2015 (2015) 1–11, https://doi.org/10.1155/2015/425456.
[73] C.B. Cheah, M. Ramli, The implementation of wood waste ash as a partial cement replacement material in the production of structural grade concrete and mortar: an overview, Resour. Conserv. Recycl. 55 (2011) 669–685, https://doi.org/10.1016/j.resconrec.2011.02.002.
[74] S. Rémond, P. Pimienta, D.P. Bentz, Effects of the incorporation of Municipal Solid Waste Incineration fly ash in cement pastes and mortars, Cement Concr. Res. 32 (2002) 303–311, https://doi.org/10.1016/S0008-8846(01)00674-3.
[75] H.F.W. Taylor, Cement Chemistry, second ed., T. Telford, London, 1997.
[76] X. Fu, C. Yang, Z. Liu, W. Tao, W. Hou, X. Wu, Studies on effects of activators on properties and mechanism of hydration of sulphoaluminate cement, Cement Concr. Res. 33 (2003) 317–324, https://doi.org/10.1016/S0008-8846(02)00954-7.
[77] D. Ndahirwa, H. Zmamou, H. Lenormand, N. Leblanc, The role of supplementary cementitious materials in hydration, durability and shrinkage of cement-based materials, their environmental and economic benefits: a review, Cleaner Materials 5 (2022) 100123, https://doi.org/10.1016/j.clema.2022.100123.